

# Differential Mueller-Matrix Tomography of the Polycrystalline Structure of Histological Sections in the Histological Determination of the Limitation of the Damage Formation of Human Internal Organs

A. Litvinenko<sup>1</sup>, I. Savka<sup>1</sup>, Yu. Ushenko<sup>2</sup>, A. Dubolazov<sup>2\*</sup>, O. Wanchulyak<sup>1</sup>,  
V. Gantyuk<sup>2</sup>, M. Talakh<sup>2</sup>, Lin Bin<sup>3</sup>, Chen Zhebo<sup>3</sup>

<sup>1</sup> Bukovinian State Medical University, 3 Theatral Sq., Chernivtsi, Ukraine, 58000

<sup>2</sup> Chernivtsi National University, 2 Kotsiubynskiyi Str., Chernivtsi, Ukraine, 58012

<sup>3</sup> Research Institute of Zhejiang University-Taizhou, 38 Zheda Road, Hangzhou, People's Republic of China, Zhejiang Province, 310027

[a.dubolazov@chnu.edu.ua](mailto:a.dubolazov@chnu.edu.ua)

## ABSTRACT

This manuscript presents the results of algorithmic testing of digital histological investigation of the duration of kidney tissue damage based on polarization reconstruction of linear birefringence maps of protein fibrillar networks. The relationships between the temporary change in the magnitude of the statistical moments of the 1st - 4th orders of magnitude characterizing the distribution of the degree of crystallization of histological sections of the kidney and the duration of damage are determined.

**Keywords:** Mueller-matrix tomography, diagnostics, Stokes vector, phase-inhomogeneous object.

## 1. Introduction

Development of a set of objective forensic medical criteria to expand the functionality and improve the accuracy of establishing the limitation of damage to internal organs according to multi-parameter digital histological examination of kidney tissue through the integrated use of polarization mapping<sup>1-5</sup> and reconstruction (tomography)<sup>6-9</sup> of the polycrystalline structure of prototypes based on statistical analysis of the temporal dynamics of changes in topographic structure of the histological sections crystallization degree of.

To describe the processes of transformation of the polarization structure of optical radiation by partial optically anisotropic layers, the following algorithm was obtained<sup>10-12</sup> in terms of the parameters of the Stokes vector  $S = \{S_1; S_2; S_3; S_4\}$

$$\frac{dS}{dr} = \{M\}(r)S(r). \quad (1)$$

Here  $\{M\}(r)$  - differential Mueller matrix;  $S(r)$  - Stokes vector of optical radiation at a distance  $r$  in a medium.

To represent the optical properties of an anisotropic medium using the formalism of the Mueller matrix, expression (1) takes the following form<sup>2</sup>

$$\frac{d\{F\}(r)}{dr} = \{F\}(r)\{M\}(r), \quad (2)$$

where  $\{F\}(r)$  - Mueller matrix of a phase-inhomogeneous object in the plane of the partial layer located at a distance  $r$ . For single scattering (non-depolarizing) layers, the symmetry of the differential matrix  $\{M\}(r)$  is a combination of six polarization properties<sup>3</sup>.

$$\{M\} = \begin{pmatrix} 0 & m_{12} & m_{13} & m_{14} \\ m_{21} & 0 & m_{23} & -m_{24} \\ m_{31} & -m_{32} & 0 & m_{34} \\ m_{41} & m_{42} & -m_{43} & 0 \end{pmatrix} = \begin{pmatrix} 0 & LD_{0,90} & LD_{45,135} & CD \\ LD_{0,90} & 0 & CB & -LB_{45,135} \\ LD_{45,135} & -CB & 0 & LB_{0,90} \\ CD & LB_{45,135} & -LB_{0,90} & 0 \end{pmatrix}. \quad (3)$$

Here  $LD_{0,90}$  and  $LB_{0,90}$  - linear dichroism and birefringence for the direction of the optical axis  $\rho = 0^\circ$ ;  $LD_{45,135}$  and  $LB_{45,135}$  - linear dichroism and birefringence for the direction of the optical axis  $\rho = 45^\circ$ ;  $CD$  and  $CB$  - circular dichroism and birefringence.

In what follows, we will use the generalized linear birefringence parameters to analyze the optical anisotropy of the polycrystalline structure of biological layers ( $LB$ )

$$LB = \sqrt{LB_{0,90}^2 + LB_{45,135}^2}. \quad (4)$$

## 2. Results and discussion

### 2.1. Maps of linear birefringence of histological sections of biological tissues of internal organs

In fragments of fig. 1 are presented examples of polarization reconstruction of the degree of crystallization of the substance of the histological section of the kidney of a deceased from coronary heart disease.

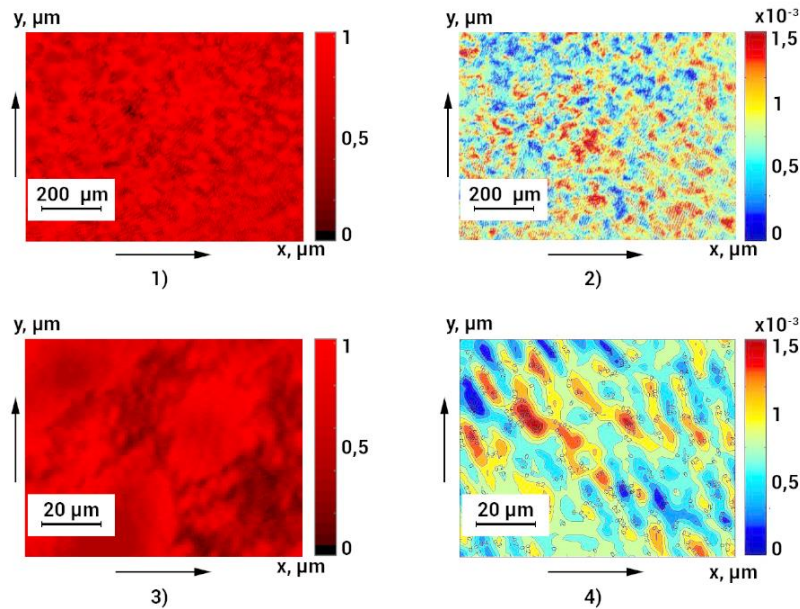


**Fig. 1.** Microscopic images ((1), (3)) and linear birefringence maps ((2), (4)) of a histological section of the kidney of a person who died from coronary heart disease.

Comparison (Fig. 1) of traditional microscopic images ((1), (3)) and tomographic reproduced maps of linear birefringence of fibrillar structures ((2), (4)) of the histological section specimen revealed the presence of a significant range of variation and coordinate inhomogeneity of the degree of tissue crystallization the kidneys.

The information thus obtained makes it possible to directly detect (inaccessible to traditional light microscopy methods) and quantify the changes in the spatial structure of the fibrillar networks of the morphological structure of tissues of the internal organs of a person as a result of traumatic injuries of various prescriptions.

### Maps of circular birefringence of histological sections of biological tissues of human internal organs

On Figure 2 are illustrated another type of optical anisotropy map - circular birefringence (fragments (2), (4)) of optically active molecular complexes of the histological section material of a kidney from a coronary heart disease.

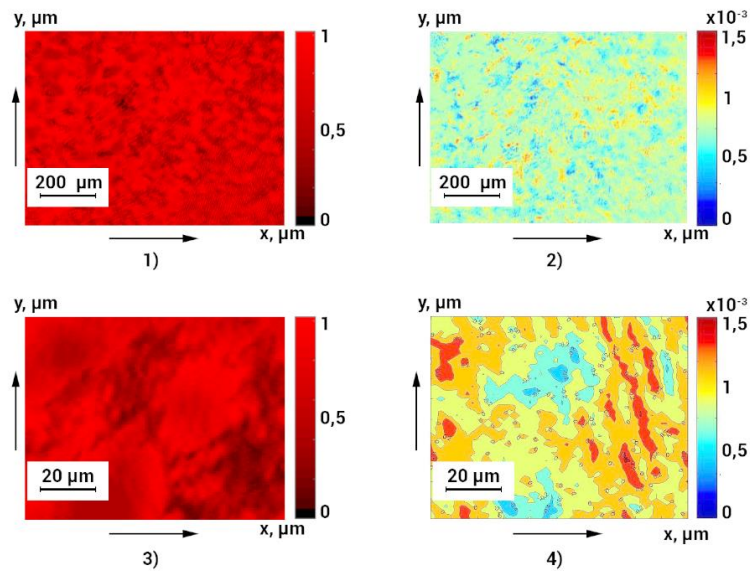


**Fig. 2.** Microscopic images ((1), (3)) and maps of circular birefringence ((2), (4)) of a histological section of the kidney of a person who died from coronary heart disease.

Thus, the polarization tomography technique opens up the possibility of a comprehensive analysis of the structural and biochemical properties of the substance of samples of biological tissues of human internal organs. Due to this, new objective diagnostic parameters will be determined and the damage limitation established.

The results of polarization tomography of digital histological studies of large-scale (40x) topographic maps of linear birefringence of histological sections of the kidney are shown in Fig.3.

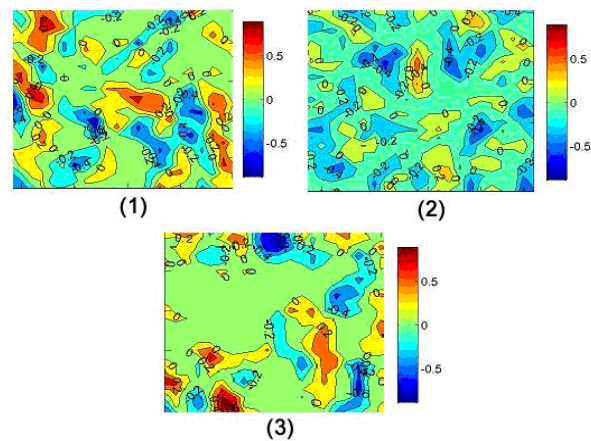


**Fig. 3.** Maps of the distributions of linear birefringence (x40) of histological sections of the kidney of the dead from the control group (1), research groups with different damage durations (6 hours - (2)) and (18 hours - (3)).

An analysis of the results of large-scale polarization reconstruction of the degree of crystallization of kidney samples revealed:

- the average distribution of the degree of crystallization is two linear intervals of 1 hour - 24 hours. and 24 hours - 48 hours and a range of variation of the eigenvalues of 0.045;
- dispersion of the distribution of the degree of crystallization — a linear interval of 24 hours and a range of variation of the eigenvalues of 0.27;
- asymmetry of the distribution of the degree of crystallization - two linear intervals of 1 hour - 24 hours and 24 hours - 72 hours and a range of variation of the eigenvalues of 2.14;
- excess of the distribution of the degree of crystallization - two linear intervals of 1 hour - 24 hours and 24 hours - 72 hours and a range of variation of the eigenvalues of 2.99.

**Table 1.** Temporal dynamics of changes in statistical moments of the 1st - 4th orders characterizing the distribution of the magnitude of the linear birefringence (40x) of histological sections of the kidney

<i>T</i> , hours	<b>2</b>	<b>4</b>	<b>6</b>	<b>12</b>	<b>18</b>
$SM_1 \times 10^{-3}$	0,78 ± 0,024	0,71 ± 0,021	0,63 ± 0,019	0,49 ± 0,013	0,35 ± 0,011
<i>p</i>	$p \pi 0,05$				
$SM_2 \times 10^{-3}$	0,69 ± 0,019	0,61 ± 0,018	0,53 ± 0,016	0,37 ± 0,014	0,21 ± 0,011
<i>p</i>	$p \pi 0,05$				
$SM_3$	0,75 ± 0,025	0,94 ± 0,037	1,13 ± 0,041	1,51 ± 0,062	1,74 ± 0,076
<i>p</i>	$p \pi 0,05$				
$SM_4$	1,07 ± 0,041	1,38 ± 0,059	1,62 ± 0,061	1,88 ± 0,073	2,21 ± 0,099
<i>p</i>	$p \pi 0,05$				
<i>T</i> , hours.	<b>24</b>	<b>48</b>	<b>72</b>	<b>96</b>	<b>120</b>
$SM_1 \times 10^{-3}$	0.21 ± 0,009	0,07 ± 0,002	0,06 ± 0,002	0,05 ± 0,002	0,04 ± 0,002
<i>p</i>	$p \pi 0,05$		$p \phi 0,05$		
$SM_2 \times 10^{-3}$	0,05 ± 0,002	0,05 ± 0,003	0,03 ± 0,002	0,04 ± 0,002	0,03 ± 0,002
<i>p</i>	$p \pi 0,05$	$p \phi 0,05$			
$SM_3$	1,92 ± 0,083	2,12 ± 0,097	2,46 ± 0,11	2,35 ± 0,11	2,42 ± 0,12
<i>p</i>	$p \pi 0,05$			$p \phi 0,05$	
$SM_4$	2,47 ± 0,11	2,76 ± 0,11	3,08 ± 0,14	3,13 ± 0,13	3,19 ± 0,15
<i>p</i>	$p \pi 0,05$			$p \phi 0,05$	

**Table 2.** Time intervals and accuracy of the method for reconstructing the polycrystalline structure of histological sections of kidney tissue

Statistical moments	Interval, hours		Accuracy, min.	
	4x	40x	4x	40x
Increase	1-24	1-24	45	35
	24-48	24-72	55	45
Dispersion	1-24	1-24	45	35
	24-48	24-72	55	45
Asymmetry	1-24	1-24	35	25
	24-72	24-120	50	45
Excess	1-24	1-24	35	25
	24-72	24-120	50	45

## Conclusions

This method is aimed at differentiating the manifestations of optical anisotropy of samples very close in morphological structure that are found in a damage formations of human internal organs. Therefore, the achieved level of accuracy ( $A_c = 77,8\%$ ) in terms of evidence-based medicine corresponds to a good level.

## References

- [1]. Ushenko, A.G., Dubolazov, O.V., Bachynsky, V.T., Peresunko, A.P., Vanchulyak, O.Y., "On the feasibilities of using the wavelet analysis of mueller matrix images of biological crystals," (2010) *Advances in Optical Technologies*, 162832.
- [2]. Zabolotna, N.I., Wojcik, W., Pavlov, S.V., Ushenko, O.G., Suleimenov, B., "Diagnostics of pathologically changed birefringent networks by means of phase Mueller matrix tomography," (2013) *Proceedings of SPIE - The International Society for Optical Engineering*, 8698, 86980.
- [3]. Ushenko, A.G., "Correlation Processing and Wavelet Analysis of Polarization Images of Biological Tissues," (2001) *Optics and Spectroscopy (English translation of Optika i Spektroskopiya)*, 91 (5), pp. 773-778.
- [4]. Ushenko, A.G., Ermolenko, S.B., Burkovets, D.N., Ushenko, Yu.A., "Polarization microstructure of laser radiation scattered by optically active biotissues," (1999) *Optika i Spektroskopiya*, 87 (3), pp. 470-474.
- [5]. Ushenko, A.G., Dubolazov, A.V., Ushenko, V.A., Novakovskaya, O.Y., "Statistical analysis of polarization-inhomogeneous Fourier spectra of laser radiation scattered by human skin in the tasks of differentiation of benign and malignant formations," (2016) *Journal of Biomedical Optics*, 21 (7), 071110.
- [6]. Bekshaev AY, Angelsky OV, Sviridova SV, Zenkova CY. Mechanical action of inhomogeneously polarized optical fields and detection of the internal energy flows. *Adv Opt Technol* 2011.
- [7]. Angelsky, O. V., Maksimyak, P. P., & Perun, T. O. (1993). Optical correlation method for measuring spatial complexity in optical fields. *Optics Letters*, 18(2), 90-92.
- [8]. Angelsky, O. V., Bekshaev, A. Y. A., Maksimyak, P. P., Maksimyak, A. P., & Hanson, S. G. (2018). Low-temperature laser-stimulated controllable generation of micro-bubbles in a water suspension of absorptive colloid particles. *Optics Express*, 26(11), 13995-14009.
- [9]. Angelsky, O. V. (2007). Optical correlation techniques and applications. *Optical correlation techniques and applications* (pp. 1-270)
- [10]. R. Ossikovski, V. Devlaminck, " General criterion for the physical realizability of the differential Mueller matrix," *Opt. Lett.* 39, 1216-1219 (2014).
- [11]. V. Devlaminck and R. Ossikovski, "Uniqueness of the differential Mueller matrix of uniform homogeneous media," *Opt. Lett.* 39, 3149-3152 (2014).
- [12]. V. Devlaminck, "Physical model of differential Mueller matrix for depolarizing uniform media," *J. Opt. Soc. Am.* 30, 2196-2204 (2013) .